Microporous and Mesoporous Materials 298 (2020) 110063

Contents lists available at ScienceDirect

Microporous and Mesoporous Materials

journal homepage: http://www.elsevier.com/locate/micromeso

A facile synthetic route and dual function of network luminescent porous polyester and copolyester containing porphyrin moiety for metal ions sensor and dyes adsorption

Kamal I. Aly [a,**], Marwa M. Sayed [a,b], Mohamed Gamal Mohamed [a,c,*], Shiao Wei Kuo [c], Osama Younis [b,d]

[a] Polymer Research Laboratory, Chemistry Department, Faculty of Science, Assiut University, Assiut, 71516, Egypt
[b] Chemistry Department, Faculty of Science, The New Valley University, El-Kharja, 72511, Egypt
[c] Department of Materials and Optoelectronic Science, Center for Functional Polymers and Supramolecular Materials, National Sun Yat-Sen University, Kaohsiung, Taiwan
[d] Department of Applied Chemistry, College of Life Sciences, Ritsumeikan University, Kusatsu, 525-8577, Japan

ARTICLE INFO

Keywords:
Porphyrin molecule
Thermal stability
Porous materials
Metal ion senor
Dyes adsorption

ABSTRACT

In this work, A novel optical metal ion sensor microporous polyesters and copolyesters containing porphyrin moiety as a monomeric unit in the main chain were successfully prepared by the interfacial condensation polymerization from 5,10,15,20-Tetrakis(4-hydroxyphenyl) porphyrin (Por-OH) and 5,10,15,20-Tetrakis(4-hydroxy-3-methoxyphenyl) porphyrin (Por-V) with aliphatic and aromatic acid chlorides derivatives (such as; adipoyl chloride, and azobenzene-4,4′-dicarboxylic chloride, respectively). These polyesters and copolyesters are characterized by FT-IR, thermogravimetric analysis (TGA), differential scanning calorimetry (DSC), X-ray diffraction, UV–Visible absorbance, fluorescence emission, and SEM measurements. The results show that our novel compounds are amorphous, have good thermal stability with high char yield and possess peaks similar to the porphynoid structure that make them good metal ion sensors with different metals ions (such as; Zn^{+2}, Cu^{+2}, Ni^{+2}, $Co^{+2,}$ and Fe^{+3}). Also, they can be used as dye adsorbents in aqueous solution and displayed amazing adsorption and selectivity toward cationic dye methylene blue (MB) over anionic sunset yellow (SY) in the dye's mixture.

1. Introduction

Porphyrin moiety is a hydrophobic, hetero macrocyclic organic compound consists of tetrapyrrole rings joined together through the methylene bridge at their α positions, so the substitution at its boundary is versatile by altering the place and changing the functional groups for structural modifications to develop the hydrophilicity leading to numerous important molecules. The high conjugation of this molecule and distinctive capability towards metals resulting in large promising applications, especially in the optoelectronic field [1,2]. This molecule and its derivatives have a unique ability to assemble into various architectures like 2D or 3D impart the property of versatile geometry aggregation nanostructure, which is the main requirement for nanotechnology applications [3]. Applications and merits, as the great importance and exciting physical and chemical properties of the polymer molecule, can curiously boost the porphyrins activities and enlarge their application fields [4–6]. Porphyrins unit can be a pendant group in the chain of a polymer or maybe a basic monomeric unit in the polymer, regarding its position in the chain. The extraordinary light gathering features, electronic, optical characteristics and easily charge transfer of porphyrin molecules make it a good sensing material [7,8]. As known that the chemosensor is a chemical species produces a measurable and reversible signal about the binding changes in the analyte, and from this definition, the optical sensor is assigned through the recognition of the changes in the optical character of the sensitive molecule. Optical properties of porphyrin molecules and their chelating ability to different metals with their wide range of chemical modifications give them the most valuable and interesting capability as prominent sensors. The

* Corresponding author. Polymer Research Laboratory, Chemistry Department, Faculty of Science, Assiut University, Assiut, 71516, Egypt.
** Corresponding author.
E-mail addresses: Kamalaly@aun.edu.eg (K.I. Aly), mgamal.eldin12@yahoo.com (M.G. Mohamed).

https://doi.org/10.1016/j.micromeso.2020.110063
Received 22 November 2019; Received in revised form 11 January 2020; Accepted 1 February 2020
Available online 5 February 2020
1387-1811/

amazing aggregation property of the porphyrin molecule and its polymers give them the porous structure that can be widely used in adsorption and catalysis [9–11]. A polymer containing a porphyrin unit is a sort of porous organic polymer connected by a strong covalent bond between porphyrin molecules [12]. These polymers hold a great building structural diversity, porosity, thermal, chemical stability and perfect adsorption property toward aromatic molecules due to their high conjugation [5,13–15]. To sustain and make environment green, researchers have recently focused on the treatment of industrial waste, including wastewater and waste gas, the increasing investigation of industry-leading to the observation of organic dyes in wastewater [16]. It is worth noting that organic dyes scattered in the natural water environment can not only seriously damage aquatic organisms [17], but also carcinogenic and teratogenic to humans. The adsorption method is the most suitable dynamic and successful decontamination strategy used [18], then the other methods, which arouses the development of multi-functional porous adsorbents. The strength and adsorption capacity of porous organic polymers (POPs) is more favorable and has received widespread attention in waste handling, which requires the development of new POPs structure and discovering a universal method to develop the adsorption power of POPs by means of composition adaptation [19–21]. In this paper, a new network polyester and copolyesters based on tetrakis hydroxy porphyrin(5,10,15,20-tetrakis (4-hydroxyphenyl) porphyrin (Por-OH) and of 5,10,15,20-Tetrakis (4-hydroxy-3-methoxy phenyl) porphyrin Por-V) as monomeric units with aliphatic and aromatic diacid chloride by the interfacial condensation polymerization. According to their photophysical properties, these polymers can serve as metal ion sensors for different metals and their structures exhibit a great adsorptivity and selectivity towards different dye molecules.

2. Experimental section

2.1. Reagents and solvents

Pyrrole (Alfa Aesar), 4-hydroxy benzaldehyde, 4-hydroxyl-3-methoxy benzaldehyde (El Nasser chemicals), 4-nitrobenzoic acid, glucose, thionyl chloride, adipoyl chloride, benzyl triethyl ammonium chloride (BTC) (Merck), methylene blue dye, colorant sunset yellow dye (Al Gomhouria Co.), zinc acetate, ferric (III) chloride anhydrous, copper (II) acetate hydrate, hexahydrate cobalt (II) chloride, nickel (II) sulfate, ethanol, sulfuric acid H_2SO_4, methanol, dimethylformamide (DMF), dimethyl sulfoxide (DMSO), Acetone, ethanol, methanol, acetic acid, glacial acetic acid, dichloromethane (CH_2Cl_2), chloroform ($CHCl_3$), nitrobenzene, propionic acid, petroleum ether (60–80°C) and petroleum ether (40–60°C) were obtained from Sigma-Aldrich and used without purification.

2.2. Measurements

Shimadzu 2110 PC scanning spectrometers for infrared spectroscopy (IR) analysis using the KBr method. Proton magnetic resonance (^{1}HNMR) and ^{13}C magnetic resonance (^{13}C NMR) spectra were obtained with an INOVA 500 using DMSO-d_6 and $CDCl_3$ as solvents. TA Q-50 Thermal Analyzer for thermogravimetric analysis (TGA) at a rate of 10 °C/min at N_2. Differential scanning calorimetry (DSC) was done with TAQ-20 under N_2. UV–Vis spectra were measured using a Shimadzu mini 1240 spectrophotometer. The fluorescent emission spectra were performed at ambient temperature through a monochromatic source of Xe light. The surface morphology of the selected samples was taken by utilizing a Jeol JSM-5400 LV scanning electron microscope (SEM) apparatus. WAXD analysis was measured using the BL17A1 wiggler beamline of the National Synchrotron Radiation Research Center (NSRRC), Taiwan, with a wavelength (λ) of 1.33001 Å used for the monochromated beam based on a triangular bent Si (111) single crystal. The BET method was used to measure the specific surface areas, pore size distributions, and pore volumes from the adsorption branches of the isotherms.

2.3. Synthesis of 5,10,15,20-Tetrakis(4-hydroxyphenyl) porphyrin (Por-OH) [18,19]

In a three-neck flask, about 250 ml with a condenser and a stirrer, a mixture of solvents nitrobenzene (20 ml), 40 ml of propionic acid and 20 ml of glacial acetic acid were refluxed during 30 min. 4-Hydroxybenzaldehyde (455 mg, 3.73 mmol) is dissolved in 25 ml of propionic acid, and allowed to dropwise in the reaction mixture. 250 mg (3.73 mmol) of pyrrole is mixed with 20 ml of nitrobenzene and the pyrrole solution is dropped slowly into the reaction mixture. The time of reflux is about 1.5 h and the reaction mixture was cooled to room temperature. Then, 50 ml of petroleum ether was added (40–60 °C) and kept the reaction mixture in the fridge overnight. The purification is done by using silica column chromatography with size (100–200 mesh) and the eluent is chloroform followed by 25% methanol in chloroform to afford Por-OH as brilliant dark blue color crystals (355 mg, 56%). ^{1}H NMR (500 MHz, $CHCl_3$-d_6, δ, ppm): 9.86 (s, 4H, $ArOH_a$), 7.83 (d, 8H, ArH_b), 7.24 (d, 8H, ArH_c), 6.96 (s, $8H_d$, βH), 3.5 (s, $2H_e$, NH). ^{13}C NMR (125 MHz, DMSO-d_6, δ, ppm): 164 (C–N), 157 (C–OH), 150, 117 and 120 (β C), 130 (ArC 3,5) and 115 (ArC 2,6).

2.4. Synthesis of 5,10,15,20-Tetrakis (4-hydroxy-3-methoxy phenyl) porphyrin (Por-V) [18,19]

In 250 ml two-necked bottom flask, 4-hydroxyl-3-methoxybenzaldehyde (1720 mg, 10 mmol) was dissolved in 75 ml of propionic acid. Then, the solution of pyrrole (700 mg, 10.45 mmol) in 40 ml of propionic acid was added to the reaction mixture and refluxed for 30 min. The reaction solution was cooled and left overnight in the fridge. The precipitate is filtrated and rinsed with petroleum ether (40–60 °C). Silica column is used to purify the solid precipitate by using ethyl acetate and hexane mixture as an eluent to give Por-V as a purple solid (495 mg, 24.8%). ^{1}H NMR (500 MHz, $CHCl_3$-d_6, δ, ppm): 9.5 (s, 4H, $ArOH_a$), 8.5 (s, $8H_b$, βH), 7.5 (d, 8H, ArH_c 3), 7.24 (d, 8H, ArH_d 2,6), 3.9 (s, $12H_e$, OCH_3) and 2.99 (s, NH). ^{13}C NMR (125 MHz, DMSO-d_6, δ, ppm): 155 (C–N), 149 (C–O–C), 157 (C–OH), 134, 120, 114 (β C), 148, 117 (ArC 3,5), 113, 110, 115 (ArC 2,6) and 56 (4 CH_3).

2.5. Synthesis of azobenzene-4, 4′-dicarboxylic Acid (Azo-COOH) [22–24]

A mixture of *p*-nitrobenzoic acid (13 g) and sodium hydroxide (50 g) in 225 ml of distilled water were warmed to 50°C. The aqueous solution of glucose (100 g in 150 ml of water) was slowly to the reaction mixture and the mixture was kept at 50 °C until the light-yellow solid was formed (8 g); m. p. 286°C.

2.6. Synthesis of azobenzene- 4,4′-dicarboxylchloride (Azo-Cl) [22–26]

In 250 ml one-necked bottom flask, Azo-COOH was heated with an excess amount of thionyl chloride for 24 h. The precipitate was formed by dilution with light petroleum and the crude product was purified by crystallization using light petroleum (60–80°C) to afford Azo-Cl as red needles, m. p. 164°C.

2.7. Synthesis of polyesters and copolyesters containing porphyrin unit

In a three-necked round-bottomed flask about 500 ml, provided with a mechanical stirrer with the speed of (2000 rev/min), dry nitrogen and a dropping funnel, 1 mmol of Por-OH or Por-V monomers were dissolved in 30 ml of dichloromethane with an amount of aqueous NaOH (5 mmol) and 0.5 g of tertiary ammonium salt benzyl triethyl ammonium chloride (BTC) were mixed for about 30 min. After mixing, 30 ml of dry

methylene chloride solution of 4 mmol of Azo-Cl or adipoyl chloride added slowly through the dropping funnel. The reaction mixture was stirred for 5 h and the polyester or copolyester was precipitated and separated by filtration, washed with hot acetone and followed by hot methanol.

2.8. Preparation of polyester and copolyester solution with different metal ions

The concentration of metal ions solution for UV and fluorescence measurement was $1x10^{-5}$ M of zinc acetate anhydrous, copper (II) acetate hydrate, nickel (II) sulfate hexahydrate, cobalt (II) chloride hexahydrate and ferric chloride anhydrous, and concentration of polyester or copolyester sample was $1x10^{-5}$ M in DMSO as solvent.

2.9. Carbonization and activation process by using KOH for polyester 1 and copolyester VI

The polyester I and copolyester VI samples were calcined in an oven at 600 °C with a heating rate of 5 °C/min for 2 h under N_2, after calcination; the material was mixed with an aqueous solution of KOH in a ratio of (KOH/powder about 2:1 (w/w)) at ordinary temperature for 24 h, the water was removed, and then activated the samples at 700 °C under N_2 flow for 6 h. The solid powder was rinsed frequently with deionized water till the filtrate solution becomes neutral pH about ~7, then dry at 120 °C.

2.10. Preparation of methylene blue dye solution

The stock solution of methylene blue is prepared with a concentration of about $2x10^{-5}$ M at (pH = 9) in a pure water at room temperature, the solution of NaOH ($5x10^{-2}$ M) and HCl ($5x10^{-2}$ M) were prepared for controlling the pH of the solution. From the stock solution, a series of the diluted solution was prepared for the calibration curve.

2.11. Preparation of colorant sunset yellow FCF dye solution

A solution of colorant sunset yellow dye with an initial concentration (2×10^{-5} M), at ambient temperature (pH = 13) was prepared. For adjusting the sunset yellow solution by using NaOH (5×10^{-2} M) and HCl (5×10^{-2} M). After preparing the Stock solution; a series of diluted solutions were prepared for the calibration curve.

2.12. Preparation of mixed dye solutions

For the dye adsorption study of a dual mixture, a series of mixture containing two dyes, methylene blue solution (2×10^{-5} M) was mixed with sunset yellow (2×10^{-5} M) solution with ratios (10:90, 20:80, 30:70, 40:60, 50:50, 60:40, 70:30, 80:20, 90:10) for a calibration curve.

2.13. Preparation of single dye solution containing adsorbent

Dried polymer adsorbent (1 mg) from all polyesters and copolyesters samples were placed in 50 ml of (2×10^{-5} M) dye solution separately, then by a syringe about 5 ml aliquot parts were transferred and measured by UV spectroscopy periodically at different time.

2.14. Preparation of binary dye solution containing adsorbent

Dried 1 mg of polyester I and copolyester VI samples before and after carbonization and activation processes were placed in 50 ml of each (2×10^{-5} M, 25 ml of methylene blue: 2×10^{-5} M, 25 ml of sunset yellow as dyes solution). Then by a syringe, about 5 ml of aliquot parts was transferred and measured by UV spectroscopy periodically at different times.

3. Results and discussion

3.1. Synthesis of Por-OH, Por-V, polyesters, and copolyesters containing porphyrin unit

The Por-OH was prepared by refluxing pyrrole with 4-hydroxybenzaldehyde in the presence of propionic acid (EtCOOH), glacial acetic acid (AcOH) and nitrobenzene ($PhNO_2$) for 1.5 h. While Por-V was prepared by refluxing pyrrole with vanillin in propionic acid as a solvent for 30 min as displayed in Scheme S1. The chemical structures of these monomers were confirmed by FTIR and NMR analyses. Fig. S1 shows the FT-IR spectra of Por-OH and Por-V. The FTIR spectrum of Por-OH showed peaks at 1597, 3150, and 3300 cm^{-1} corresponds to C═N vibration, N–H stretching bond, and a hydroxyl group. While, the peaks appeared at 1600, 3150 and 3361 cm^{-1} for Por-V. Fig. S2 displays the ^1H NMR spectra of Por-OH and Por-V in $CHCl_3$-d_6. As shown in Fig. S2(a), Por-OH showed the characteristic signals at 9.86 and 6.96 ppm for the OH group and βH of porphyrin molecule, respectively. Por-V exhibited signals for the phenolic OH at 9.5 ppm, 3.9 ppm for methoxy group (OCH_3), and for βH at 8.5 ppm [Fig. S2(b)]. The ^{13}C NMR spectra of Por-OH and Por-V in DMSO-d_6 are shown in Fig. S3. The spectrum of Por-OH [Fig. S3(a)] displayed signals in the range 117–150 ppm for (βC) and 157 ppm for C–OH in the phenyl ring, while ^{13}C NMR spectrum of Por-V [Fig. S3(b)] exhibited (βC) signals in the range 114–134 ppm and 149 ppm for methoxy group. Azo-COOH monomer was prepared from 4-nitrobenzoic acid in alkali solution and hot glucose solution in the presence of glacial acetic acid. Then, Azo-COOH was refluxed with an excess amount of thionyl chloride to give Azo-Cl as displayed in Scheme S2. The FT-IR spectrum of Azo-Cl [Fig. S4] showed a vibration peak at 1779 cm^{-1} for the CO–Cl. The polyesters (I-IV) and copolyesters (V-VI) are prepared by the interfacial polymerization of por-OH or por-V with Azo-Cl or adipoyl chloride in the presence benzyl triethylammonium chloride (BTC) as a catalyst, as depicted in Scheme 1 and Scheme 2.

The FT-IR spectra [Fig. 1] displayed that all polyesters and copolyesters have a new band around 1740 cm^{-1} assigned for the carbonyl ester groups and C═C stretching at 1590-1600 cm^{-1}. The interference of the C═C ring stretching with –N═N- absorption band of the aromatic azo [27–31], Also, the peaks at 1250–1260, 850 and 764, 3444 and 3050 cm^{-1} which are assigned to C–O–C bonds (ether link), out the plane vibration of aromatic hydrogen, N–H stretching of a pyrrole ring, and C–H aromatic, respectively [32]. We found that the homopolymers and copolymers materials were partially dissolved in dimethyl sulfoxide and do not soluble in DMF as well as NMP and dimethylacetamide (DMAc). As known that the increase in the molecular weight and crosslinking degree of polymers lead to decrease solubility and inhibit the interaction between polymer chains and solvent molecules and preventing those polymer chains from being transported into solution [27,33–35].

3.2. X-ray analysis

The crystalline properties of polyester I, polyester IV and copolyester VI were examined by XRD measurement as displayed in Fig. 2. For polyester I which contains azo group, the XRD pattern of polyester I has some sharp peaks, and this indicates that this polymer has semi-crystalline structure. While, XRD profile of polyester IV and copolyester VI show a sharp peak with a broad peak, as an indication of semi-crystalline, the reason for this peak is the presence of alkyl chain which imparts a kind of flexibility of the polymer chain [28–30,34,35].

3.3. SEM images

The surface morphology of polyester I and copolyester VI were investigated by SEM images at different magnification [Fig. 3(a-d)]. The SEM images of polyester I [Fig. 3(a) and (b)] show that the surface is harsh and tough and seems like assembled layers or plates which is

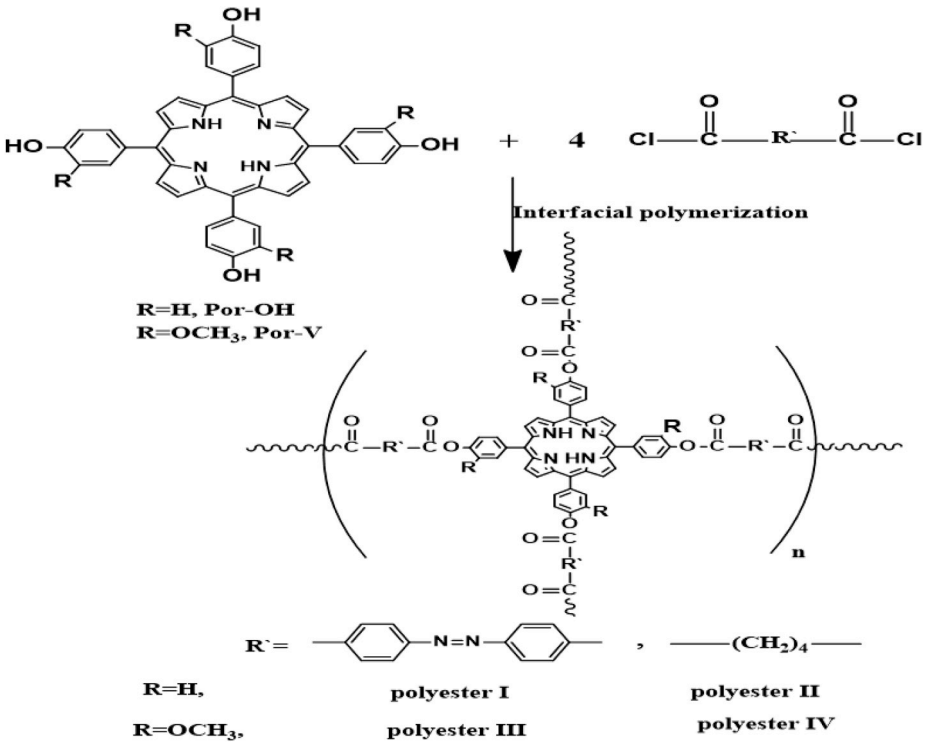

Scheme 1. Synthesis of porphyrin polyesters (I-IV).

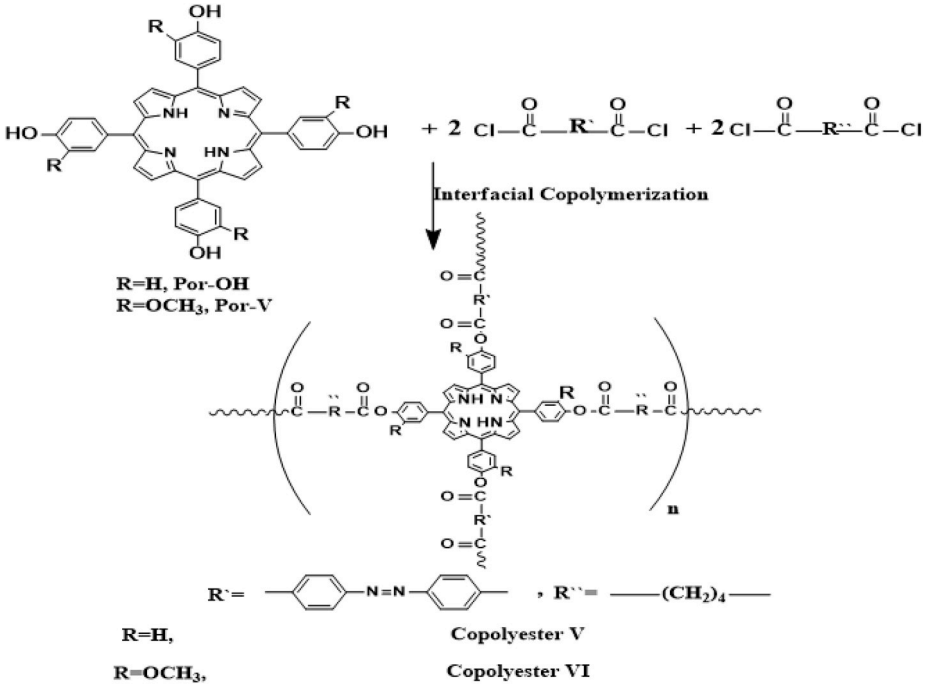

Scheme 2. Synthesis of porphyrin copolyesters (V-VI).

attributed to the presence of azo moiety leads to assembling of monomer units as layers. On the contrary, copolyester VI are different and has spongy structure [Fig. 3(c) and (d)], as a result of the presence of alkyl chain from adipoyl moiety giving a suitable distance between the monomeric unit [31,32,36,37].

3.4. TGA and DSC analyses of polyester and copolyesters containing porphyrin unit

The thermogravimetric analysis (TGA) and differential scanning calorimetry (DSC) were carried out to investigate the thermal stability properties of the synthesized polyesters and copolyesters containing porphyrin unit as presented in Table S1, Fig. 4 and Fig. 5. TGA profile [Fig. 4] of polyesters and copolyesters shows that the thermal

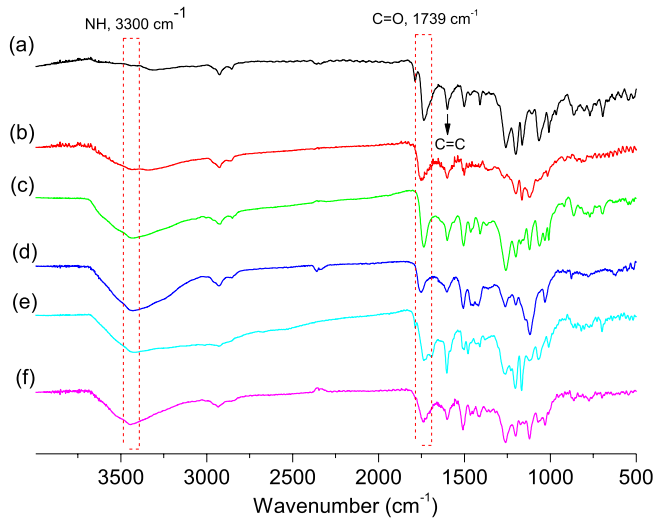

Fig. 1. FT-IR spectra of polyester (I-IV) from (a) to (d), and (e, f) for copolyesters (V-VI).

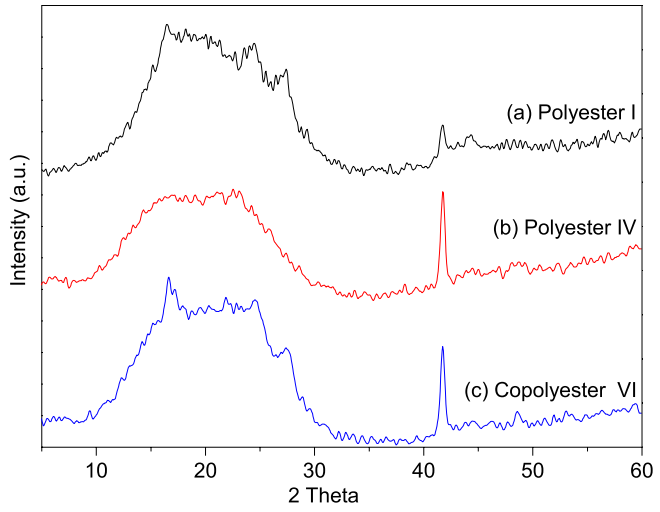

Fig. 2. X-ray diffractions of polyesters I, IV and copolyester V.

degradation temperature (Td_{10}) was in the range 243–309 °C. Based on TGA analysis, we observed that polyester I possess the highest char yield and highest decomposition temperature compared to other samples. The values of thermal degradation temperature (Td_{10}) and char yield were summarized in Table S1.

Fig. 5 shows DSC analysis for polyesters and copolyesters were performed at heating rate 20 °C/min under a N_2 atmosphere. In the DSC profile, there were no crystallization or melting peaks for these polymers or copolymers. The T_g values of some selected samples are summarized in Table S1. The values of the glass transition temperature (T_g) of polyesters and copolyesters were around 104–108 °C, indicating that our polymers possess a highly crosslinked density [38]. Also, the T_g values of the polymer containing tetrakis(4-hydroxyphenyl) porphyrin monomer are smaller in comparison with those obtained from polymers containing tetrakis (4-hydroxy-3-methoxyphenyl) porphyrin monomer, this indicates that the methoxy group acts as a hard segment and retards the movement of the polymer chains [39].

3.5. UV and fluorescence behavior of polyester and copolyesters

UV absorbance and fluorescence emission are effective ways of monitoring the optical properties, through immobilization of the

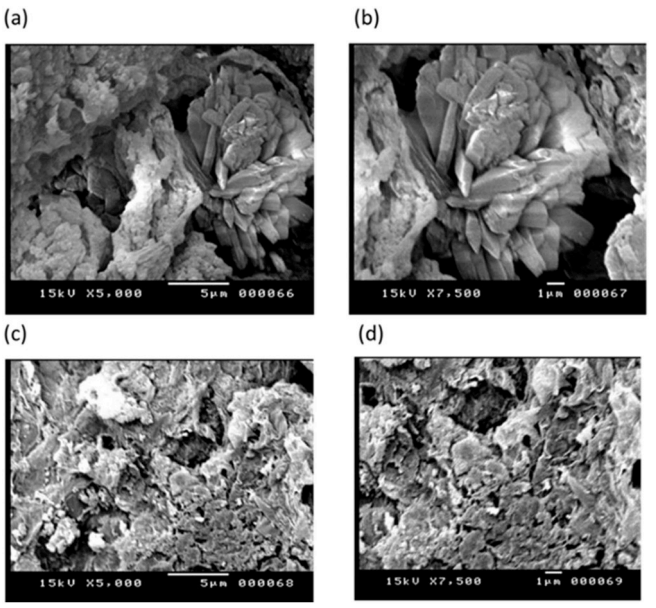

Fig. 3. SEM images of polyester (I) (a,*b*) and copolyester (VI) (c, d) at different magnifications (a,c at X = 5000) and (b,d at X = 7500).

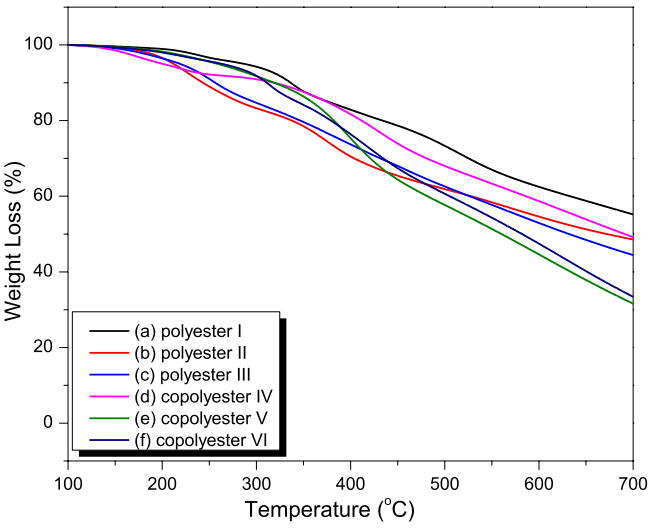

Fig. 4. TGA curves of polyesters I, II, III, IV, and copolyesters V and VI.

material in a liquid state or solid phase to support its reaction with light. Macrocyclic sensing materials, including porphyrins, act as a diverse developing platform. Their abundant characteristics can be employed to indicate their reaction with host compounds: their chromophore nature, an adjustable chelating framework, and a large π-aromatic system. Generally, the donating ability is reduced when an electron-donating (ED) group binds metal ion and converts the nature of the system from donating to accepting, as the conjugation is minimized and the absorption intensity is decreased [40,41]. The electromagnetic spectrum of porphyrins displays two distinguished spectrum area in UV–visible region and have five diagnostic bands; Soret bands are strong (also known as B bands) at 380–500 nm, is referred to moving and interference of the free electron pairs of the pyrrole, the other bands are weak called Q bands between 500 and 700 nm and assigned to the charge transitions from carbons of the pyrrole rings to macrocyclic atoms [42]. From UV–vis absorbance spectra [Fig. S5], the molecules without a methoxy group exhibit a high absorption in the sorbet band around 426 nm and those which have an azo group in their structure, show an

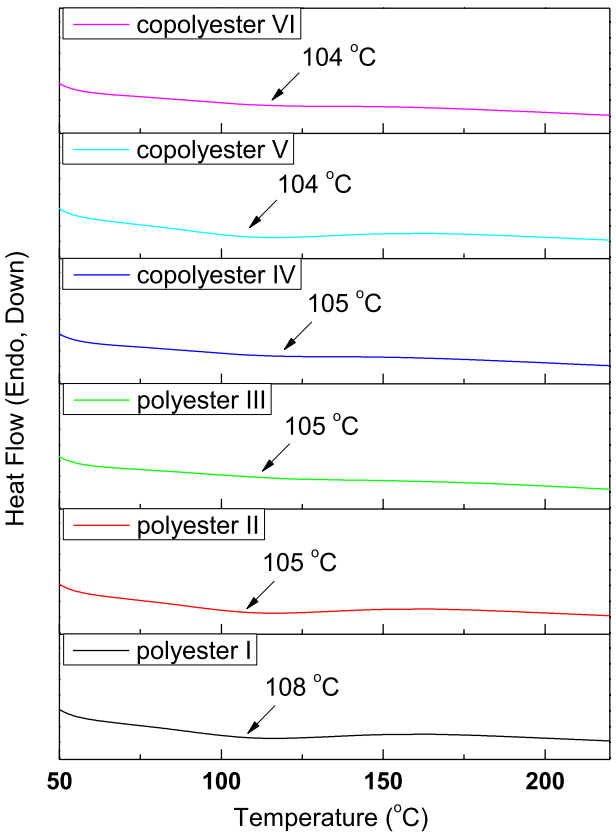

Fig. 5. DSC profile of polyester I, II, III and copolyester IV and VI.

absorption peak at 334 nm related to this group. In polyesters and copolyesters materials upon appropriate metalation with different metals produce flexibly tunable electronic, optical and redox properties. Occurring of irregular absorption is an indication of the strong interaction between electrons of the ring and the central metal. For polyester I with Zn^{+2} and Fe^{+3} ions cause a red shift, while the rest of metal ions cause a blue shift. polyester II with Zn^{+2} ions causes a red shift. polyester III with Zn^{+2} and Co^{+2} ions cause a small red shift. For polyester IV, there is no observance of a sorbet peak. While, copolyester V with Ni^{+2}, $Co^{+2,}$ and Zn^{+2} ions cause a red shift in wavelength. Furthermore, it is well known that metal ions coordinate in the center of porphyrins to form metal-to-metal or metal-to-ligand electron transfer [43]. Also, we used PL measurements to investigate the metal ions sensor's ability for each polyester and copolyesters towards specific metal ions. The normal fluorescence spectrum of porphyrin indicates the possibility of two spectral bands, including the Q band, and the phosphorescence spectral band. Figs. 6 and 7 display the fluorescence spectra of the polyester I, II, III, and IV, copolyester V and VI with different metal ions. The fluorescence spectra of all these materials show the abroad band at 651–664 nm which is attributed to the hindered macrocycle. The reliance of fluorescent signal strength on the characteristic organic group connected to the lattice results in a change in the electron's nature surrounding the porphyrin. The polymers which contain hydrogen atom facilitate the emission process of the porphyrin molecules than those that contain methoxy group in the chain. Also, the emission decrease with samples that have an azo group in their backbone as a result of conjugation and sharing electrons of porphyrin structure and hence decrease their intensities. The photoluminescence color of polyesters, copolyesters with metals ions was evaluated quantitatively with (CIE) chromaticity diagram [Fig. S6 and Table S2], results display that for polyester I, polyester II and copolyester V providing CIE coordinates of (x, y) = (0.71, 0.29) and nearly the same for other metals confirming the production of red emission except for Zn^{+2} and Cu^{+2} metals ions have coordinates of (x, y)= (0.66, 0.33) releasing reddish-orange emission, thus these polymers can be used for deduction of Zn^{+2} and Cu^{+2} ions. For polyester III (0.69, 0.31) indicating red color emission of that polymer and also for its metal's ions except for Zn^{+2}, Cu^{+2} and Co^{+2} ions have coordinates releasing reddish-orange emission, thus these polymers can be used for deduction of Zn^{+2} and Cu^{+2}, for polyester IV (0.25,

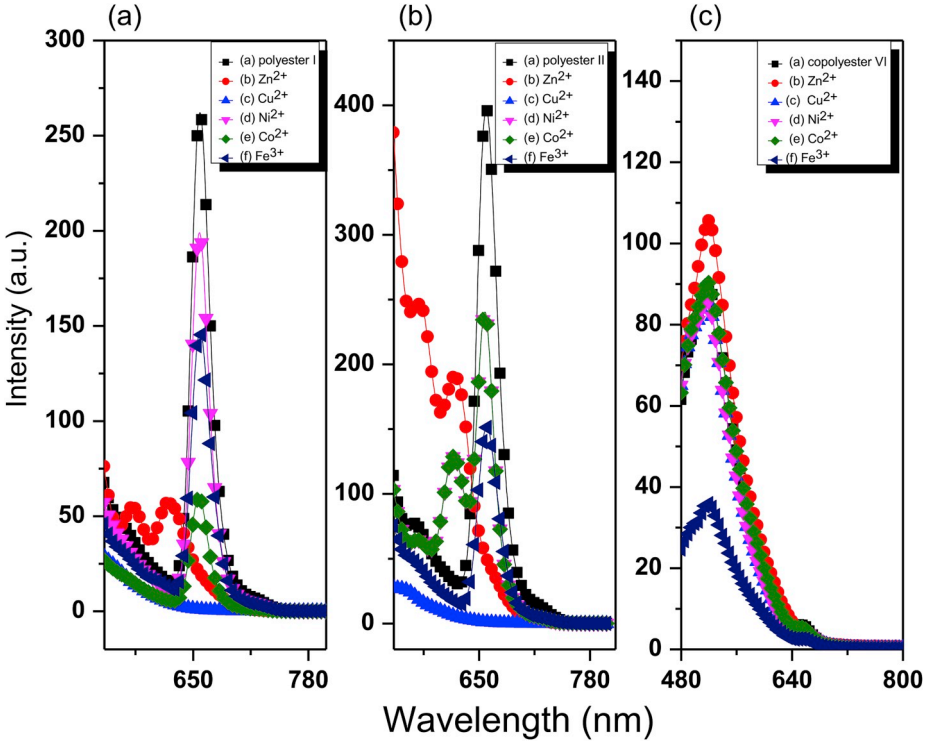

Fig. 6. PL spectra of polymers with different metal ions of (a) polyester I, (b) polyester II and (c) copolyester VI in DMSO.

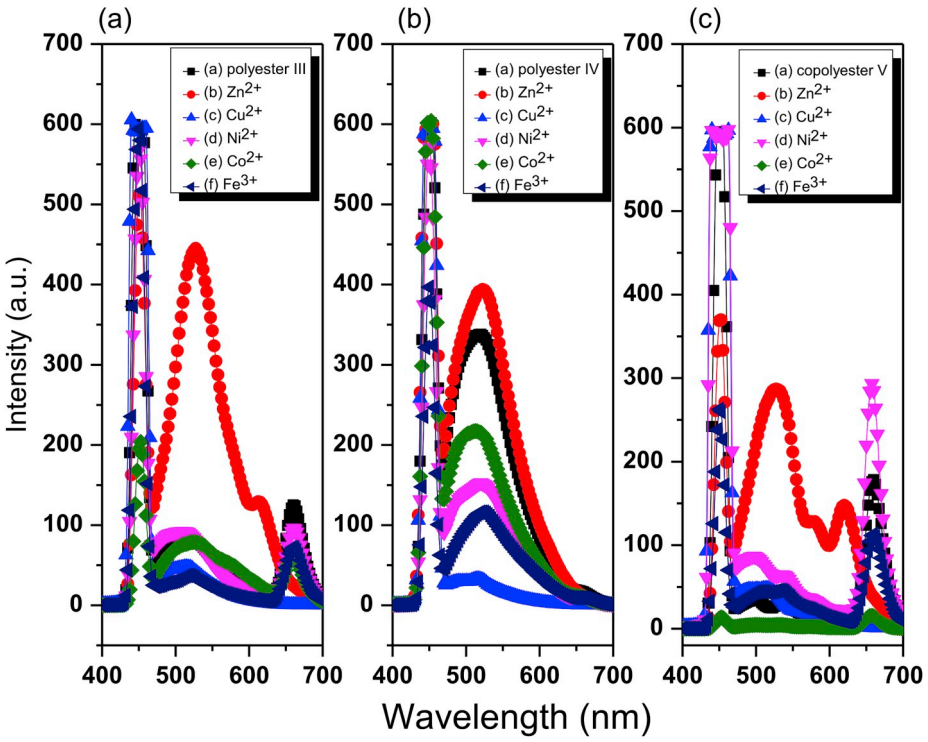

Fig. 7. PL spectra of polymers with different metal ions of (a) polyester III, (b) polyester IV and (c) copolyester V in DMSO.

0.49) at 519 nm, indicating light green color emission and also for all metals ions except Cu^{+2}, it has coordinates releasing blue-green emission, thus polyester IV can be used for deduction of Cu^{+2} ions. In addition, copolyester VI has CIE coordinates (0.24, 0.41) at 515 nm, indicating green color emission and also for Co^{+2} ions, while Fe^{+3} and Zn^{+2} ions (0.20, 0.27) and (0.22, 0.34) exhibiting blue-green color. For Cu^{+2} and Ni^{+2} ions have coordinates of (x, y)= (0.21, 0.36) releasing bluish-green emission. These results indicate that the methoxy group in the porphynoid structure with a flexible chain of adipoyl molecules without the azo group in the backbone of the polymer can alter and suppress porphyrin emission.

3.6. Dye adsorption application

The adsorption behaviors of polyester I, III, IV and copolyester VI toward MB, SY, and mixtures of them were investigated by using UV–Vis absorbance measurements [Figs. 8 and 9]. The capability of polyesters and copolyesters to adsorb dye molecules from solution is measured quantitatively by observing the change in UV–Vis absorbance spectra of the MB alkaline solution (pH = 9) at 665 nm, and SY dye solution (pH = 13) at 443 nm, respectively. The adsorption capacity (q) of adsorbents was calculated from equation (1):

$$q=((C_0-C_t)*V)/m \quad (1)$$

Where V is the taken volume of adsorbed solution in (L), m is the quantified weight of adsorbents in (g), C_0 is the start concentration and C_t is the residual concentration in (mg/L) of dye solution. Calibration curves of MB dye, SY dye and a binary mixture of two dyes are made to determine and monitor the concentration of dye solution [Fig. S7]. From the obtained results [Tables S3, S4, and Figs S8 and S9], two general tendencies can be concluded: the two molecular dyes are hydrophilic, cationic (MB) and anionic (SY). The solution of single (MB) dye becomes faint, illustrating that polyesters I, IV, copolyesters V and VI have the capability to adsorb (MB) molecules in a distinct manner. We observed that polyesters containing adipoyl moiety and copolyesters containing a methoxy group have a faster adsorption affinity. The variance in adsorptive is due to the chemistry of the adsorbent surface [44–48]. The organic dye adsorption process comprises two mechanisms, including electrostatic strength, and diffusive interactions. The low adsorptivity of the molecule is due to its size and spatial distribution. Large molecules could not be able to permeate easily inside the small pores, the aggregation and accumulation of these huge molecules at the top surface of small pores result in pore blocking, inhibition of additional mass transfer and low adsorption [49]. From the surface area measurements; the BET surface area and pore size of polyester I were 83.33 m^2/g and 3.21 nm. While, the BET surface area and pore size of copolyester VI were 75.12 m^2/g and 3.26 nm [Fig. S10]. These two materials exhibit quick adsorption of (MB) molecules and no change in the SY solution.

However, the color darkens, which means that SY's absorption is very limited. Since anionic dye (SY) will produce in aqueous solution an ionic (SO^{3-}) ion [50]. Observations of no dye adsorption in the presence of sulfites or sulfates confirmed the participation of (SY) sulfonate groups in the adsorption process [51].

$$D{-}{-}SO_3Na \rightarrow D{-}{-}SO^{3-} + Na^+$$

The reason for this big variance is the mutual influence of dye charge and adsorbent molecules. The partially negative oxygen atom in the carbonyl group is responsible for the electrostatic repulsion between the dye molecules and adsorbent surface, causing finite adsorption and giving a rise in the intensity of the peak at 337 nm corresponding to the azo group of the dye molecule. This also explains the affinity of adsorption of this molecular (SY) dye after carbonization and activation process as the atom that is responsible for this repulsion is disappeared, the resulting attraction is only between the carbon of adsorbent and nitrogen atoms of the dye molecule in the mixture after activation [44, 52,53]. The aqueous MB may contain various forms of its molecules and appears clearly in its UV absorption spectrum, with peaks at 664 nm for single ($MB+$), 612 nm for dimers [$(MB+)_2$] and 556 nm for higher aggregates of MB [$(MB+)_n$]. These forms of the molecule are connected by some forces like hydrophobic interactions, hydrogen bonding, Van Der Waals forces, London dispersion, and other short-range forces by keeping charges as far as possible. The ratio between the absorbance at 666

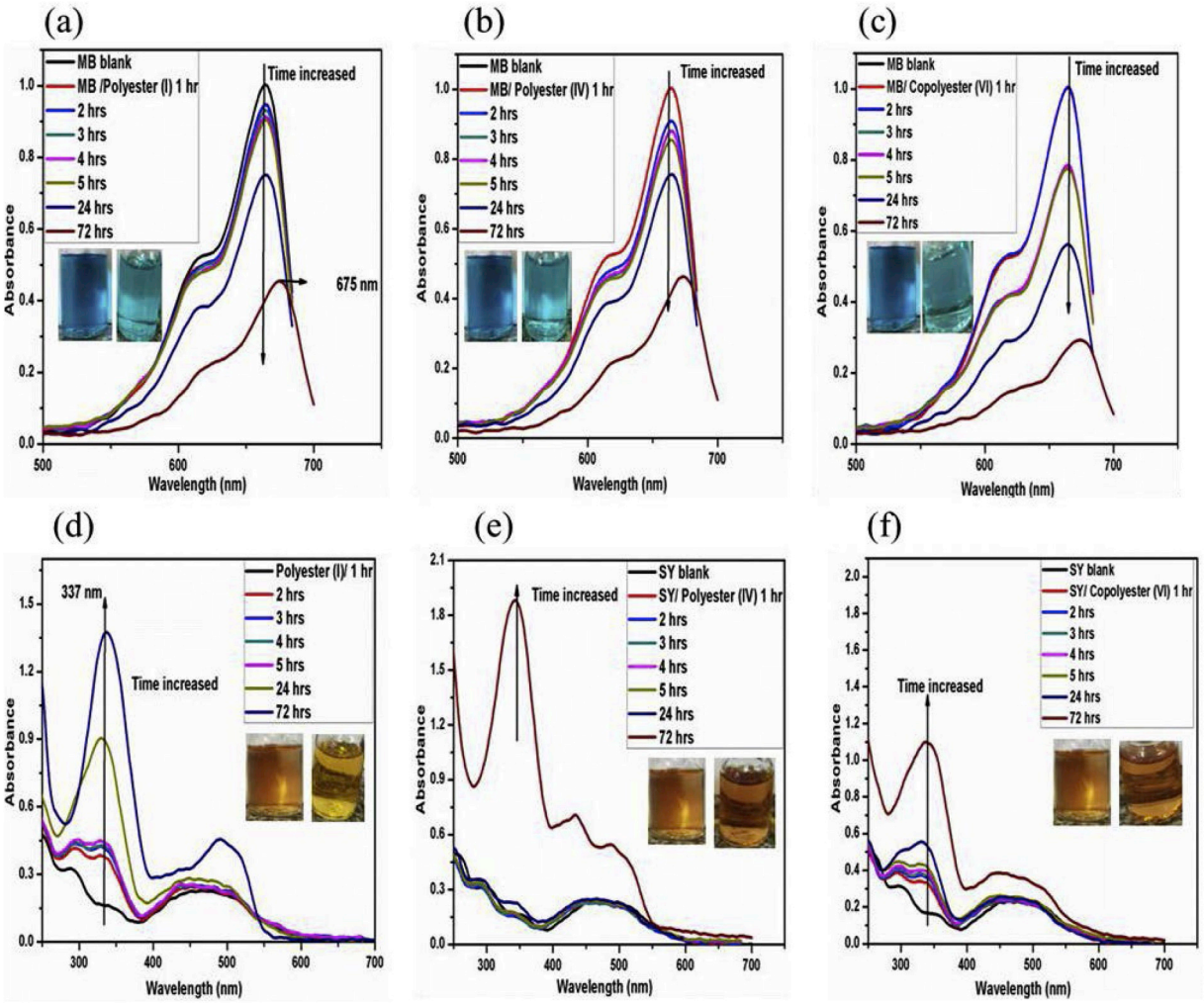

Fig. 8. UV–vis spectra of single (MB) solution (a,b,c) and single (SY) solution (d,e,f) adsorption recorded at various times, (a,d) for polyester I, (b,e) for polyester IV and (c,f) for copolyester VI, inset images are of solution left before and right after adsorption for each 1 h.

and 612 nm of MB is minimized by raising the concentration of MB. This suggests the dependence of MB absorption on its concentration produced from the equilibrium between the forms of MB single and dimer [54]. In the presence of adsorbents polyesters (I-IV) or copolyesters, the absorption peak of MB has slightly shifted to a longer wavelength of about 10 nm. In the mixture solution as the concentration of adsorbents is increased, the absorption of the MB monomer peak is increased, and the dimer peak is decreased. This may be referred to that the dimer form is suppressed by the inclusion of the single MB molecules inside the pores of polymers preventing dye molecules from aggregation and dimerization. The selectivity in adsorption is easily demonstrated from a mixture of MB and SY, the mixture is green exhibits two distinguished absorbance peaks; at 420 nm and at 640 nm. Experiments with a mixture of cation and anion dye are complicated by precipitation of the mixture with opposite charges. However, the preference adsorption of one substance causes another substance to dissolve from the sediment, so the color change of the solution is proven of selectivity. In the mixture of two dyes adsorbent before activation shows higher adsorption, and appear clearly when the volume of solution is reduced from 1 to 0.50, the decrease in the amount of adsorbed dyes is more significant and almost reached the maximum, resulting in the formation of an orange solution by dissolving the yellow dye solution when blue dye was adsorbed. Adsorbent after activation in the system contains an equal concentration of the two dyes the interaction is obvious, as in a single dye system the adsorption capability is noticeable. While in binary systems the lower adsorptive dye in the single-component system is preferred to be adsorbed. The existence of MB dye enhances the affinity of SY dye towards adsorbent [55]. The peak strength at 612 nm begins to increase, and the peak at 664 nm decreases, indicating a significant increase in the A612/A664 ratio and $(MB)_2$ formation/aggregation was caused by the presence of activated polymer molecules. The dimer formation is also confirmed by the peak at 620 nm known as isosbestic and shifted to a shorter wavelength when the concentration of MB is increased. As the electrostatic forces among MB are decreased by ion-pair complexes of MB with activated polymers, so the molecules tend to approach each other more closely [56]. Moreover, the medium becomes hydrophobic due to the structural effects of water [57,58]. This is the decrease in surface area after the activation process by KOH. For example, the BET surface area of activated polyester I and copolyester VI were 27.04 and 9.84 m^2/g, respectively [Fig. S11]. Carbon activation is the most important step in producing AC because it raises the porosity and surface area of the product. When the activation temperature is high, strong gasification reactions might result in destroying micropore structure by breaking down or merging, and formation of mesopore volume [59]. The higher activation temperature makes reactions between steam and carbon is controlled by diffusion, violent and thus caused a nonhomogeneous reaction in the particle, so the reaction occurs on their surfaces that have a little contribution to the pore generation. Furthermore, widen the pores and convert some micropores into mesopores and macropores, minimizing the surface area, pore volume

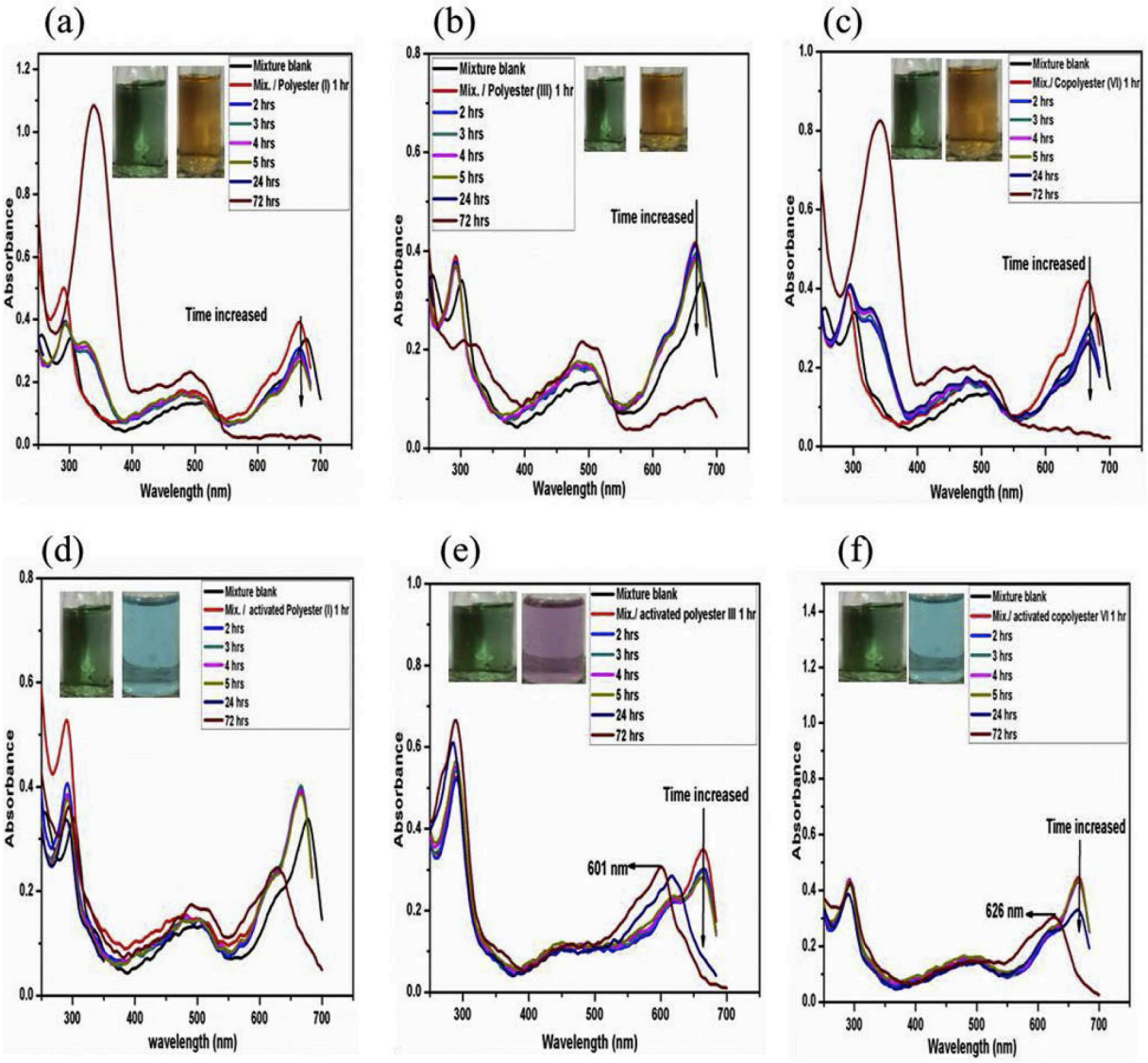

Fig. 9. UV–Vis spectra of binary mixture (MB) and (SY) solution adsorption recorded at various times, (a,b,c) before activation and (d,e,f) after activation, (a, d) for polyester I, (b, e) for polyester III and (c, f) for copolyester VI, inset images are of solution left before and right after adsorption for each one.

and increasing ash formation [60].

4. Conclusions

In conclusion, the novel polyesters and copolyesters containing porphyrin unit as repeating units in the polymer chain have been successfully prepared by the interfacial polycondensation method. The resulting polymers are characterized by different analyses techniques such as FT-IR, TGA, DSC, X-ray diffraction, SEM, UV–Vis absorbance and emission spectroscopy. These new polymers possess a high glass temperature and good thermal stability based on TGA and DSC analyses. Because of porphyrin moiety, these novel polymers can be used to detect metal ions (Zn^{+2}, Cu^{+2}, Ni^{+2}, $Co^{+2,}$ and Fe^{+3}) in solution. Also, they show amazing adsorption and selectivity toward cationic dye MB over anionic dye SY.

Declaration of competing interest

The authors declare that they have no known competing financial interests or personal relationships that could have appeared to influence the work reported in this paper.

CRediT authorship contribution statement

Kamal I. Aly: Supervision, Investigation, Formal analysis, Writing - original draft. **Marwa M. Sayed:** Investigation, Writing - original draft. **Mohamed Gamal Mohamed:** Supervision, Investigation, Formal analysis, Writing - original draft, Writing - review & editing. **Shiao Wei Kuo:** Supervision, Investigation, Formal analysis, Writing - original draft. **Osama Younis:** Supervision, Investigation, Formal analysis, Writing - original draft.

Acknowledgments

The authors are grateful to the Research Funding Unit at the Faculty of Science, Assiut University (Egypt), for financial support.

Appendix A. Supplementary data

Supplementary data to this article can be found online at https://doi.org/10.1016/j.micromeso.2020.110063.

References

[1] D. Wohrle, The colours of life, softcover, £49.50, in: L.R. Milgrom (Ed.), An Introduction to the Chemistry of Porphyrins and Related Compounds, vol. iOxford university press, Oxford, 1997, ISBN 019-855380-3, p. 225. Advanced Materials, 9 (1997) 1191-1192.

[2] G. Mukherjee, J. Thote, H.B. Aiyappa, S. Kandambeth, S. Banerjee, K. Vanka, R. Banerjee, A porous porphyrin organic polymer (PPOP) for visible light triggered hydrogen production, Chem. Commun. 53 (2017) 4461–4464.

[3] M. Evyapan, A.D.F. Dunbar, Controlling surface adsorption to enhance the selectivity of porphyrin-based gas sensors, Appl. Surf. Sci. 362 (2016) 191–201.

[4] C. Escudero, J. Crusats, I. Díez-Pérez, Z. El-Hachemi, J.M. Ribó, Folding and hydrodynamic forces in J-aggregates of 5-Phenyl-10,15,20-tris(4-sulfophenyl) porphyrin, Angew. Chem. Int. Ed. 45 (2006) 8032–8035.

[5] X. Liu, H. Li, Y. Zhang, B. Xu, S. A, H. Xia, Y. Mu, Enhanced carbon dioxide uptake by metalloporphyrin-based microporous covalent triazine framework, Polym. Chem. 4 (2013) 2445–2448.

[6] M. Takeuchi, S. Tanaka, S. Shinkai, On the influence of porphyrin π–π stacking on supramolecular chirality created in the porphyrin-based twisted tape structure, Chem. Commun. (2005) 5539–5541.

[7] A. Mahmood, J.-Y. Hu, B. Xiao, A. Tang, X. Wang, E. Zhou, Recent progress in porphyrin-based materials for organic solar cells, J. Mater. Chem. 6 (2018) 16769–16797.

[8] D. Chen, C. Liu, J. Tang, L. Luo, G. Yu, Fluorescent porous organic polymers, Polym. Chem. 10 (2019) 1168–1181.

[9] Q. Sun, Z. Dai, X. Meng, F.-S. Xiao, Porous polymer catalysts with hierarchical structures, Chem. Soc. Rev. 44 (2015) 6018–6034.

[10] Q. Sun, B. Aguila, G. Verma, X. Liu, Z. Dai, F. Deng, X. Meng, F.-S. Xiao, S. Ma, Superhydrophobicity: constructing homogeneous catalysts into superhydrophobic porous frameworks to protect them from hydrolytic degradation, Inside Chem. 1 (2016) 628–639.

[11] Q. Sun, Z. Dai, X. Meng, F.-S. Xiao, Homochiral porous framework as a platform for durability enhancement of molecular catalysts, Chem. Mater. 29 (2017) 5720–5726.

[12] J. Wang, C. Jiao, M. Li, X. Wang, C. Wang, Q. Wu, Z. Wang, Porphyrin based porous organic polymer modified with Fe3O4 nanoparticles as an efficient adsorbent for the enrichment of benzoylurea insecticides, Mikrochim. Acta 185 (2017) 36.

[13] X.-S. Wang, J. Liu, J.M. Bonefont, D.-Q. Yuan, P.K. Thallapally, S. Ma, A porous covalent porphyrin framework with exceptional uptake capacity of saturated hydrocarbons for oil spill cleanup, Chem. Commun. 49 (2013) 1533–1535.

[14] A.R. Oveisi, K. Zhang, A. Khorramabadi-zad, O.K. Farha, J.T. Hupp, Stable and catalytically active iron porphyrin-based porous organic polymer: activity as both a redox and Lewis acid catalyst, Sci. Rep. 5 (2015) 10621.

[15] L. Sun, Z. Liang, J. Yu, R. Xu, Luminescent microporous organic polymers containing the 1,3,5-tri(4-ethenylphenyl)benzene unit constructed by Heck coupling reaction, Polym. Chem. 4 (2013) 1932–1938.

[16] M. Rafatullah, O. Sulaiman, R. Hashim, A. Ahmad, Adsorption of methylene blue on low-cost adsorbents: a review, J. Hazard Mater. 177 (2010) 70–80.

[17] V.K. Garg, M. Amita, R. Kumar, R. Gupta, Basic dye (methylene blue) removal from simulated wastewater by adsorption using Indian Rosewood sawdust: a timber industry waste, Dyes Pigments 63 (2004) 243–250.

[18] Y. Qin, L. Wang, C. Zhao, D. Chen, Y. Ma, W. Yang, Ammonium-Functionalized hollow polymer particles as a pH-responsive adsorbent for selective removal of acid dye, ACS Appl. Mater. Interfaces 8 (2016) 16690–16698.

[19] Q. Chen, D.-P. Liu, J.-H. Zhu, B.-H. Han, Mesoporous conjugated polycarbazole with high porosity via structure tuning, Macromolecules 47 (2014) 5926–5931.

[20] V. Guillerm, Ł.J. Weseliński, M. Alkordi, M.I.H. Mohideen, Y. Belmabkhout, A. J. Cairns, M. Eddaoudi, Porous organic polymers with anchored aldehydes: a new platform for post-synthetic amine functionalization en route for enhanced CO_2 adsorption properties, Chem. Commun. 50 (2014) 1937–1940.

[21] L.-J. Feng, Q. Chen, J.-H. Zhu, D.-P. Liu, Y.-C. Zhao, B.-H. Han, Adsorption performance and catalytic activity of porous conjugated polyporphyrins via carbazole-based oxidative coupling polymerization, Polym. Chem. 5 (2014) 3081–3088.

[22] V.D. Rumyantseva, A.S. Gorshkova, A.F. Mironov, Improved method of 5,10,15,20-Tetrakis(4-hydroxyphenyl)porphyrins synthesis, Macroheterocycles 6 (2013) 59–61.

[23] Z. Sun, Y. She, R. Zhong, Synthesis of p-substituted tetraphenylporphyrins and corresponding ferric complexes with mixed-solvents method, Front. Chem. Eng. China 3 (2009) 457.

[24] D.H. Marrian, P.B. Russell, B.J.F. Hudson, J.W. Cornforth, R.H. Cornforth, W. J. Dunstan, M.L. Tomlinson, J. Chem. Soc. (1946) 753–756.

[25] M.A. Abd-Alla, K.I. Aly, A.S. Hammam, Arylidene polymers IV. Synthesis, characterization and morphology of new polyesters of diarylidenecyclohexanone, High Perform. Polym. 1 (1989) 223–237.

[26] K.I. Aly, A.S. Hammam, S.M. Radwan, M.A. Abdel-Rahman, New unsaturated copolyesters based on diarylidenecyclopentanone. Optimum conditions of synthesis, characterization and morphology, Int. J. Basic Appl. Sci. 11 (2011) 15–35.

[27] K.I. Aly, A.A. Khalaf, I.A. Alkskas, New polymer syntheses XII. Polyketones based on diarylidenecycloalkanones, Eur. Polym. J. 39 (2003) 1273–1279.

[28] K.I. Aly, New polymer syntheses XXVIII. Synthesis and thermal behavior of new organometallic polyketones and copolyketones based on diferrocenylidenecyclohexanone, J. Appl. Polym. Sci. 94 (2004) 1440–1448.

[29] M.A. Abd-alla, K.I. Aly, Arylidene polymers. IX. Synthesis, characterization, and morphology of new polyesters of diarylidenecycloalkanones containing thianthrene units, J. Macromol. Sci. Part A - Chemistry 28 (1991) 251–267.

[30] K.I. Aly, M.A. Hussein, Synthesis, characterization and corrosion inhibitive properties of new thiazole based polyamides containing diarylidenecyclohexanone moiety, Chin. J. Polym. Sci. 33 (2015) 1–13.

[31] D. Jayaprakash, L. Ravikumar, M.J. Nanjan, Synthesis of polyamides containing azo groups, Die Makromolekulare Chemie, Rapid Commun. 2 (1981) 611–615.

[32] H. Ghafuri, F. Mohammadi, R. Rahimi, E. Mohammadiyan, Synthesis and characterization of a new magnetic nanocomposite with metalloporphyrin (Co-TPyP) and sulfated tin dioxide (Fe_3O_4@SnO_2/SO_4^{2-}), and investigation of its photocatalytic effects in the degradation of Rhodamine B, RSC Adv. 6 (2016) 83947–83953.

[33] B.A. Miller-Chou, J.L. Koenig, A review of polymer dissolution, Prog. Polym. Sci. 28 (2003) 1223–1270.

[34] N.S. Al-Muaikel, K.I. Aly, M.A. Hussein, Synthesis, characterization and antimicrobial properties of new poly(ether-ketone)s and copoly(ether-ketone)s containing diarylidenecycloalkanone moieties in the main chain, J. Appl. Polym. Sci. 108 (2008) 3138–3147.

[35] M.A. Abd-alla, K.I. Aly, Arylidene polymers. XVII. Cyclization of aromatic poly [dibenzylidenecyclopentanone-hydrazide] as a route to polyheterocyclic 1,3,4-oxadiazole and 1,2,4-triazole, J. Macromol. Sci., Part A 29 (1992) 185–192.

[36] Y. Xu, Q. Yu, D. Zhao, W. Zhang, N. Wang, J. Li, Synthesis and characterization of porphyrin-based porous coordination polymers obtained by supercritical CO_2 extraction, J. Mater. Sci. 53 (2018) 10534–10542.

[37] Y. Wang, A. Wang, P. Yang, W. Hu, X. Guo, J. Zhang, C. Li, C. Zhang, A polypyrrole hybrid material self-assembled with porphyrin: facial synthesis and enhanced optical limiting properties, J. Mater. Sci. Chem. Eng. (2017) 26–43, 05.

[38] S. Ma, T. Yu, The glass transition temperature of crosslinked unsaturated polyester, J. Polym. Eng. 12 (1993) 179–196.

[39] M. Pergal, J. Dzunuzovic, S. Ostojic, M. Pergal, A. Radulovic, S. Jovanovic, Poly (urethane-siloxane)s based on hyperbranched polyester as crosslinking agent: synthesis and characterization, J. Serb. Chem. Soc. 77 (2012) 919–935.

[40] S. Huh, S.-J. Kim, Y. Kim, Porphyrinic metal–organic frameworks from custom-designed porphyrins, CrystEngComm 18 (2016) 345–368.

[41] D.A. Roberts, M.J. Crossley, S. Perrier, Fluorescent bowl-shaped nanoparticles from 'clicked' porphyrin–polymer conjugates, Polym. Chem. 5 (2014) 4016–4021.

[42] M. Gouterman, Study of the effects of substitution on the absorption spectra of porphin, J. Chem. Phys. 30 (1959) 1139–1161.

[43] T. Yamamoto, N. Fukushima, H. Nakajima, T. Maruyama, I. Yamaguchi, Synthesis and chemical properties of π-conjugated zinc porphyrin polymers with arylene and aryleneethynylene groups between zinc porphyrin units, Macromolecules 33 (2000) 5988–5994.

[44] L.R. Radovic, I.F. Silva, J.I. Ume, J.A. Menéndez, C.A.L.Y. Leon, A.W. Scaroni, An experimental and theoretical study of the adsorption of aromatics possessing electron-withdrawing and electron-donating functional groups by chemically modified activated carbons, Carbon 35 (1997) 1339–1348.

[45] J.M. Yang, R.J. Ying, C.X. Han, Q.T. Hu, H.M. Xu, J.H. Li, Q. Wang, W. Zhang, Adsorptive removal of organic dyes from aqueous solution by a Zr-based metal–organic framework: effects of Ce(III) doping, Dalton Trans. 47 (2018) 3913–3920.

[46] W. Zhang, R.Z. Zhang, Y.Q. Huang, J.M. Yang, Effect of the synergetic interplay between the electrostatic interactions, size of the dye molecules, and adsorption sites of MIL-101(Cr) on the adsorption of organic dyes from aqueous solutions, Cryst. Growth Des. 8 (2018) 7533–7540.

[47] Q. Gao, J. Xu, X.H. Bu, Recent advances about metal–organic frameworks in the removal of pollutants from wastewater, Coord. Chem. Rev. 378 (2019) 17–31.

[48] J. Zhao, Q. Huang, M. Liu, Y. Dai, J. Chen, H. Huang, Y. Wen, X. Zhu, X. Zhang, Y. Wei, Synthesis of functionalized MgAl-layered double hydroxides via modified mussel inspired chemistry and their application in organic dye adsorption, J. Colloid Interface Sci. 505 (2017) 168–177.

[49] X. Zhuang, Y. Wan, C. Feng, Y. Shen, D. Zhao, Highly efficient adsorption of bulky dye molecules in wastewater on ordered mesoporous carbons, Chem. Mater. 21 (2009) 706–716.

[50] J.L. Figueiredo, J.P.S. Sousa, C.A. Orge, M.F.R. Pereira, J.J.M. Órfão, Adsorption of dyes on carbon xerogels and templated carbons: influence of surface chemistry, Adsorption 17 (2011) 431–441.

[51] J. Bandara, J.A. Mielczarski, J. Kiwi, 1. Molecular mechanism of surface recognition. Azo dyes degradation on Fe, Ti, and Al oxides through metal sulfonate complexes, Langmuir 15 (1999) 7670–7679.

[52] W. Yi, H. Wu, H. Wang, Q. Du, Interconnectivity of macroporous hydrogels prepared via graphene oxide-stabilized pickering high internal phase emulsions, Langmuir 32 (2016) 982–990.

[53] G. Zhang, S. Shuang, C. Dong, J. Pan, Study on the interaction of methylene blue with cyclodextrin derivatives by absorption and fluorescence spectroscopy, Spectrochim. Acta Mol. Biomol. Spectrosc. 59 (2003) 2935–2941.

[54] S.J. Allen, G. McKay, J.F. Porter, Adsorption isotherm models for basic dye adsorption by peat in single and binary component systems, J. Colloid Interface Sci. 280 (2004) 322–333.

[55] A.A. Shahir, M. Rashidi-Alavijeh, S. Javadian, J. Kakemam, A. Yousefi, Molecular interaction of Congo Red with conventional and cationic gemini surfactants, Fluid Phase Equil. 305 (2011) 219–226.

[56] K. Patil, R. Pawar, P. Talap, Self-aggregation of Methylene Blue in aqueous medium and aqueous solutions of Bu_4NBr and urea, Phys. Chem. Chem. Phys. 2 (2000) 4313–4317.

[57] R. Sanan, T.S. Kang, R.K. Mahajan, Complexation, dimerisation and solubilisation of methylene blue in the presence of biamphiphilic ionic liquids: a detailed spectroscopic and electrochemical study, Phys. Chem. Chem. Phys. 16 (2014) 5667–5677.

[58] W.M.A.W. Daud, W.S.W. Ali, M.Z. Sulaiman, The effects of carbonization temperature on pore development in palm-shell-based activated carbon, Carbon 38 (2000) 1925–1932.

[59] Y. Chen, S.-R. Zhai, N. Liu, Y. Song, Q.-D. An, X.-W. Song, Dye removal of activated carbons prepared from NaOH-pretreated rice husks by low-temperature solution-processed carbonization and H_3PO_4 activation, Bioresour. Technol. 144 (2013) 401–409.

[60] H.T. Ma, H.C. Ly, V.T.T. Ho, N.B. Pham, D.C. Nguyen, K.T.D. Vo, P.D. Tuan, Effect of the carbonization and activation process on the adsorption capacity of rice husk activated carbon, Vietnam. J. Sci. Technol. 55 (2017) 494.